

ROBUSTNESS ANALYSIS OF TALL TIMBER BUILDING SUBJECTED TO COMPARTMENT FIRE

Tongchen Han¹, Solomon Tesfamariam²

ABSTRACT: The construction of tall timber buildings is gaining popularity around the world leveraging on its inherent characteristics such as renewability and high strength-to-weight ratio. However, timber is prone to fire damage due to its combustibility. The robustness of timber buildings exposed to fire is still not well understood. This paper presents the robustness analysis of a 12-story timber frame-core wall building subjected to compartment fire. First, natural fire scenarios are developed considering the combustibility of timber. Subsequently, a numerical model of the timber building is constructed and the developed building model is subjected to the natural fire after imposed dead load and live load. Finally, the structural fire performance of the building is evaluated and a framework to assess its robustness is proposed. The robustness of the designed timber building exposed to fire is quantified by calculating the robustness index considering different fire scenarios and direct failure and indirect failure caused by the fire damage.

KEYWORDS: *Tall timber building, Robustness analysis, Robustness index, Numerical simulation, Fire*

1 – INTRODUCTION

The implementation of engineering wood products, e.g., glulam, CLT [1,2], NLT, enables engineers to design larger and taller timber buildings than ever before. However, the combustibility of timber is the main reason that limits the use of timber structures, especially tall timber buildings. Although the developers were permitted to construct higher timber buildings according to the newest National Building Code of Canada (NBCC) [3], the evaluation of the fire performance of the tall timber building is still needed. This study aims to assess the robustness of a 12-story timber building under natural fire with different strategies of passive fire protection design.

1.1 MODELLING OF TIMBER STRUCTURES EXPOSED TO FIRE

A reliable and computationally efficient numerical model of the timber building is the prerequisite for the robustness evaluation. However, building-level timber structural fire model is very limited. Han and Tesfamariam [4,5] developed a simplified but accurate modelling approach for timber structural components using the equivalent section temperature (EST) method. In sequential thermal-structural analysis, instead of incorporating the whole temperature field into the structural model, the EST method simplifies the non-uniform temperature field into a single temperature value that reflects the strength/stiffness reduction of the section. The application of EST improves the flexibility of structural modelling and

reduces computational time. The structural fire model using EST method is able to be extended to the building-level, since the structural model can be developed using simple elements, which facilitates the evaluation of timber building fire performance.

1.2 NATURAL FIRE SCENARIO DESIGN

One of the primary challenges in fire design for timber structures is the contribution of exposed timber surfaces to the fire load. The fire lasted longer and the charring of timber is deeper when timber surfaces are exposed. The extended fire in turn leads to more charring. Rather than using specified parametric fire model in EN 1991-1-2 [6], which oversimplifies the decay phase of fire, it is crucial to incorporate more representative fire scenarios in the design process for timber structures. To quantify the contribution of exposed timber, various approaches were proposed based on parametric fire model [7], zone models [8], or fire dynamic models [9]. Ni et al. [10] summarized these methodologies and proposed analytical models to evaluate the HRR for timber compartment fire. Fire curves were subsequently derived using Zone model [10], with model calibration performed against an extensive experimental database. These resources provide valuable insights into the design of timber building compartment fire.

1.3 ROBUSTNESS ASSESSMENT

The robustness of the structure is to prevent the consequences spreading to a higher level in the structural

¹ Tongchen Han, School of Engineering, The University of British Columbia, Okanagan Campus, 3333 University Way, Kelowna, BC, Canada, V1V 1V7. Email: touch01@student.ubc.ca

² Solomon Tesfamariam, Department of Civil and Environmental Engineering, University of Waterloo, 200 University Ave W, Waterloo, ON N2L 3G1, Canada. Email: solomon.tesfamariam@uwaterloo.ca

scale [11]. The robustness assessment of timber structures can be conducted on different levels, e.g., material level, connector level, connection level, component level, and building level [12]. The quantification of robustness, as demonstrated by [13], is presented using different metrics related to unexposed and exposed structures, e.g., stiffness-based metrics, damage-based metrics, and energy-based metrics. Baker [14] proposed the risk-based robustness index, as calculated in (1):

$$I_{Rob} = \frac{R_{Dir}}{R_{Dir} + R_{Ind}} \tag{1}$$

where R_{Dir} and R_{Ind} are direct and indirect risks caused by the exposure. For the robustness evaluation of timber building, (1) is modified as:

$$I_{Rob} = \frac{A_{Fail,Dir}}{A_{Fail,Dir} + \sum_{i=0}^n (P(C_i|D)A_{Fail,Ind,i})} \tag{2}$$

where $A_{Fail,Dir}$ is the direct failure area; $P(C|D)$ is the collapse possibility on the condition of the damage caused by exposure; $A_{Fail, Ind}$ is the indirect failure area. Probabilistic and deterministic approaches were employed for the robustness assessment [12]. The probabilistic approach involves the calculation of collapse probability accounting for various uncertainties including material and hazard domains, which is too complicated to discuss here.

Most studies focus on the deterministic robustness evaluation of timber building, typically assuming a sudden column loss scenario [11,12], however, this assumption is unrealistic. The robustness of timber buildings exposed to fire should account for the realistic scenario and explicitly model the strength/stiffness degradation of structural components during exposure. This is based on accurate and reliable fire models and finite element models.

2 – PROTOTYPE BUILDING

The 12-story timber frame-core wall building based on the Michael Green Architecture (MGA) report [13], located in Vancouver, BC, was initially designed for seismic load. The section sizes and grades of designed components are selected based on CSA 086 [14] and shown in Table 1.

Table 1: Designed components of the building

Component	Section size (mm)	Grade
Beam in X and Y	265 x 256	D-Fir, 24f-E
Column in X and Y	365 x 532	D-Fir, 24f-E
Shear wall in X	4250 x 267	SPF, E1
Shear wall in Y	3000/5500 x 245	SPF, E1

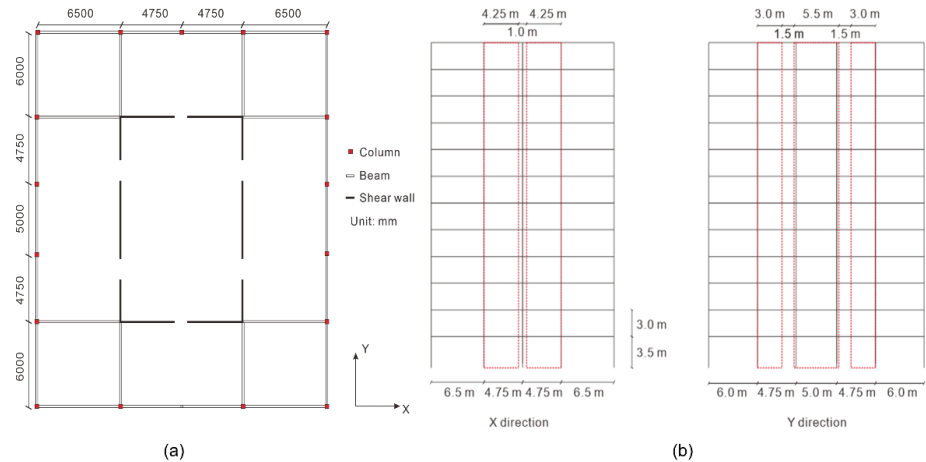


Figure 1. Layout of the building: (a) plan view and (b) elevation view.

The layout of the building is shown in Fig. 1. The plan view for each story is shown in Fig. 1(a). Each story includes four 6.5 m x 6.5 m office compartments at corners and public areas/corridors. The first story is assumed to be the public area. The first story height is 3.5 m and other story's height is 3 m. The thickness of the 5-ply CLT floor is 245 mm, with grade of SPF, E1. In the X direction, two coupled balloon-type CLT shear walls with width of 4.25 m were connected with 1.0 m coupled beam on every floor. In the Y direction, three coupled balloon-type CLT shear

walls with widths of 3 m, 5.5 m, and 3 m, respectively, were connected with 1.5 m coupled beam on every floor. The core wall system of the building was assumed to be fully protected with encapsulation layers, thereby their strengths were not damaged by fire.

3 – NATURAL FIRE DESIGN

The combustibility of timber components was considered in the design of natural fire scenario. The fire hazard was

assumed to be located at the office. The movable fuel load density of the office building can be found in EN 1991-1-2 [6], and the 80% fractile value (550 MJ/m²) was used. The additional fire load provided by the exposed timber can be calculated according to the method presented in [9]. The charring of timber can be calculated using (3) to (5) according to EN 1991-1-2 [6]:

$$d_{char,t} = 2\beta_{par}t_0 \tag{3}$$

$$\beta_{par} = 1.5\beta_n \frac{0.2\sqrt{\Gamma}-0.04}{0.16\sqrt{\Gamma}+0.08} \tag{4}$$

$$t_0 = 0.009q_t/O \tag{5}$$

where β_n is the notional design charring rate, which is 0.7 mm/min; q_t is the effective fuel load density; O is the opening factor; Γ is the time factor, see EN 1991-1-2 [6]. Once the final charring depth is known, the energy provided by the charring layer can be calculated based on Fig. 2, according to Ni et al. [10].

Since the charring layer will provide more fuel load and elongate the fire, an iterative procedure (Fig. 3) is employed to calculate the final fixed fuel load (exposed timber surface) provided by the timber. The total fuel load equals to the plus of moveable fuel load and fixed fuel load.

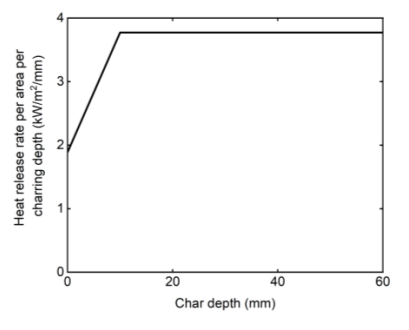


Figure 2. Heat release rate per unit area per charring depth.

The layout of the compartment is shown in Fig. 4. To consider the contribution of exposed timber surfaces to the fire, the ceiling and infill wall 1, wall 3, and wall 4 were assumed to be exposed to fire. The calculating procedure for the final charring depth and fuel load is listed in Table 2. The convergence criterion for the charring depth d_m in the procedure was assumed to be 1.5 mm.

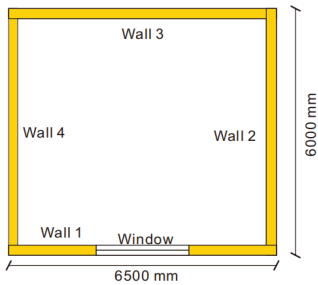


Figure 4. Designed compartment.

Table 2: Fuel load calculation

Iteration	d_{char} (mm)	$q_{t, char}$ (MJ/m ²)	t_0 (min)
0	36.3	127.7	19.5
1	22.3	84.3	12
d2	14.7	55.7	7.9
3	9.7	36.7	5.2
4	6.4	24.3	3.4
5	4.2	16.0	2.2
6	2.8	10.6	1.5
7	1.8	7.0	0.9
8	1.2	4.6	0.6

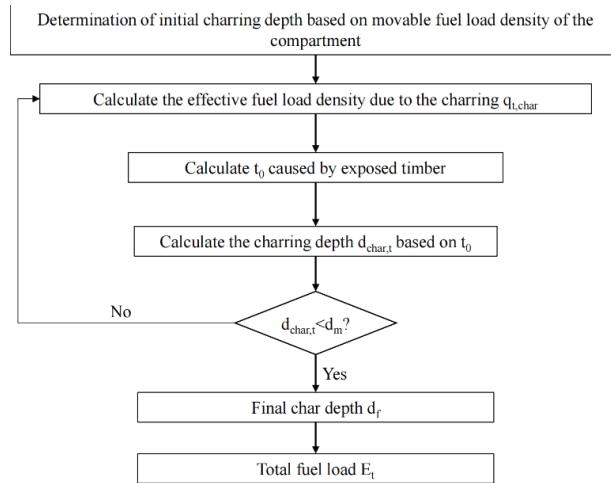


Figure 3. Iterative procedure to determine the final charring depth and fuel load.

Once the fuel load is calculated, the heat release rate (HRR) can be derived based on combustion models. Typically, two combustion models are adopted, named external flaming combustion model and extended fire duration combustion model. Based on [10], the extended fire duration combustion model (Fig. 5) was more unfavorable for timber buildings.

For fire duration combustion model, the HRR in steady phase Q_{vent} is calculated with (6)

$$Q_{\text{vent}} = \dot{m} H_{c, \text{net}} m \quad (6)$$

where m is the combustion factor, which is 0.8; $H_{c, \text{net}}$ is the net heat of combustion of timber, which is 17.5 MJ/m². \dot{m} is the coefficient and can be calculated using (7)

$$\dot{m} = k_p A_v \sqrt{h_{eq}} \quad (7)$$

where coefficient k_p can be estimated as 0.1; A_v is the total area of vertical openings on all walls; h_{eq} is the weighted average of window heights on all walls.

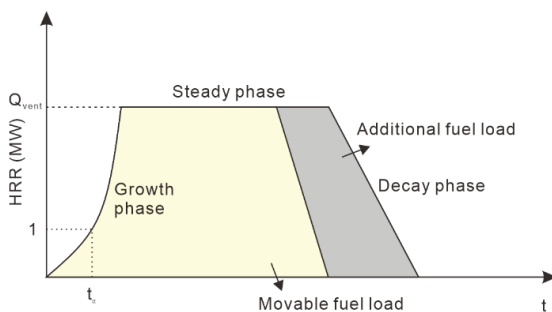
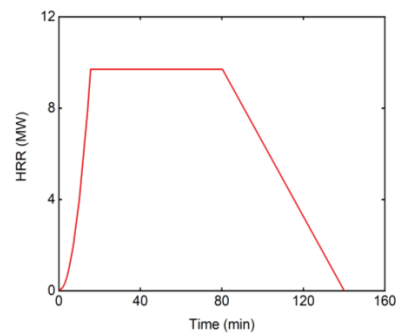
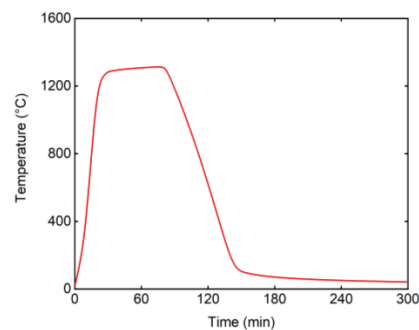


Figure 5. Extended fire duration combustion model.

The fire growth rate t_a was 300 s (medium fire growth rate). The calculated HRR curve is shown in Fig. 6(a). The fire curve (Fig. 6(b)) was calculated using one Zone model based on Ozone [15]. The fire curve was used as the input for thermal analysis in the finite element model.



(a)



(b)

Figure 6. Calculated heat release rate curve and fire curve: (a) heat release rate curve and (b) fire curve.

4 – BUILDING MODEL DEVELOPMENT

4.1 THERMAL ANALYSIS

Thermal analysis was conducted on the timber section level. The analysis was conducted in 2D using the heat transfer element DC2D4. The variations of thermal properties of timber with temperature were adopted from EN 1995-1-2 [16]. The heat flux in the model was considered by conduction q_k (see (8)), convection q_c (see (9)), and radiation q_r (see (10)):

$$q_k = -k\Delta T \quad (8)$$

$$q_c = h_c(T_g - T_s) \quad (9)$$

$$q_r = \varepsilon_m \sigma [(T_r + 273)^4 - (T_m + 273)^4] \quad (10)$$

where ΔT is the temperature gradient; k is the thermal conductivity; $h_c=25\text{ W/m}^2\text{K}$ is the heat transfer coefficient for convection; T_g is the gas temperature; T_s is the surface temperature, ε_m is the emissivity (0.8), σ is the Stephan Boltzmann constant ($\sigma=5.67 \times 10^{-8} \text{ W/m}^2\text{K}^4$), and T_r is the effective radiation temperature, $T_r = T_g$.

The equivalent section temperature (EST) method [4] was used to simplify the temperature field of the timber section derived through thermal analysis. The proposed EST method gives a single temperature value that reflects the strength or stiffness degradation of the section, and the strength or stiffness degradation during the cooling phase is also included. For the following structural analysis, the calculated EST of the timber section was input into the structural model.

4.2 STRUCTURAL ANALYSIS

The structural model of the building is shown in Fig. 7. The beam and column were modelled with B31 element and the floor was modelled with S4R element. The shear analogy method [17] was used to transform the anisotropic CLT into isotropic material that can be defined in the model. The shear analogy method assumes two virtual beams, i.e., Beam A and Beam B. Beam A was given the sum of the inherent flexural strength of the individual plies along their own neutral axes, while Beam B was given the “Steiner” points part of the flexural strength, the flexible shear strength of the panel, as well as the flexibility of all connections. These two beams were coupled with infinitely rigid web members, so that an equal deflection between Beams A and B was obtained. The bending and shear stiffnesses of Beam A and Beam B were calculated in (11) to (13)

$$(EI)_A = \sum_{i=1}^n E_i I_i = \sum_{i=1}^n E_i \frac{b_i t_i^3}{12} \quad (11)$$

$$(EI)_B = \sum_{i=1}^n E_i A_i z_i^2 \quad (12)$$

$$(GA)_B = \frac{a^2}{\frac{h_1}{2G_1 b_1} + \sum_{i=2}^{n-2} \frac{h_i}{G_i b_i} + \frac{h_n}{2G_n b_n}} \quad (13)$$

where E_i is the elastic stiffness of layer i ; I_i is the moment of inertia of layer i ; b_i is the width of layer i ; A_i is the area of layer i ; z_i is the distance from the neutral axis of layer i to the neutral axis of the section; a is the distance between the neutral axes of two outside layers; G_i is the shear stiffness of layer i ; t_i is the thickness of layer i ; n is the number of layers in CLT. The average strength of the CLT section was adopted as the strength of the isotropic material.

The bilinear curve was used to describe the stress-strain relationship of the timber. The timber beam/column strength and modulus according to CSA 086 [14] and calculated isotropic CLT strength and modulus are listed in Table 3. The strength/stiffness reduction of timber was specified according to EN 1995-1-2 [16]. The connections in the building model, i.e., beam-column connection, beam-floor connection, beam-shear wall connection, and floor-shear wall connection, were modelled with connector element CONN2D2. Specifically, two types of connectors were used, i.e., joint and rigid. For the joint connector, the two connected nodes were restrained in translational movement, and only rotations were allowed. For the rigid connector, the two connected nodes were restrained in all degrees of freedom. The bottom columns were fixed on the ground and columns in different stories were tied together. Finally, 4352 elements were generated for the structural analysis.

Table 3: Mechanical properties of structural components in the building model.

Component	Yield strength (MPa)	Modulus (MPa)
Beam/Column	30.2	12800
Floor/Shear wall	12.3	6513

The load combination including fire load was specified in NBCC [3], as shown in (14):

$$L = DL + 0.5LL + FL \quad (14)$$

where DL is the dead load; LL is the live load; FL is the fire load. The dead load was calculated based on the density of the structural/non-structural components, which was 2.8 kPa. The live load was adopted according to NBCC [3]. For the office building, the live load was 2.4 kPa. The vertical load was applied to the floor in the

building model. The dynamic, implicit solver was used for the structural analysis.

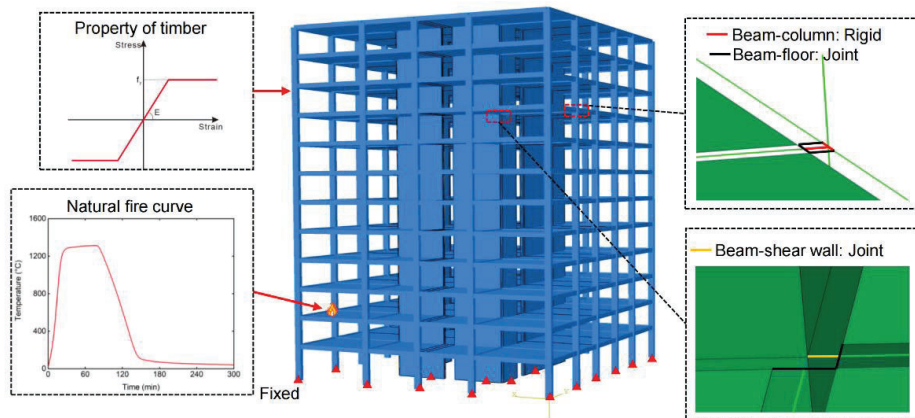


Figure 7. Structural model.

5-STRUCTURAL FIRE PERFORMANCE AND ROBUSTNESS ASSESSMENT

4.1 STRUCTURAL FIRE PERFORMANCE

The structural fire performances of the building under natural fire scenarios were evaluated and two passive fire protection strategies were considered. The first strategy (S1) assumed that no fire protections were used in the building. The second strategy (S2) assumed that diagonal columns (locations shown in Fig. 8) in the fire compartment were protected by a 15.9 mm type X gypsum board.

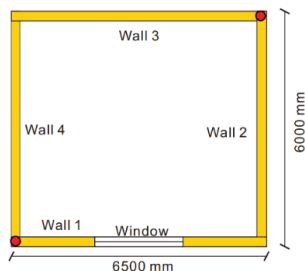


Figure 8. Location of protected column.

To present the collapse mode and displacement evolution of the building under fire, one deterministic case was illustrated. The fire was assumed to be located on the third floor.

The structural response of S1 is shown in Fig. 9. It can be seen in Fig. 9(a) that significant deformation is observed

for columns, which indicates the buckling failure at the end. It leads to the overall drop of corner compartments above the fire location. Fig. 9(b) shows the stress distribution of the building when it collapses. Due to the failure of the structural components in the exposed compartment, adjacent columns bear the redistributed load from the failure region, which leads to increased stress. Fig. 9(c) shows the displacement evolution of structural components. The displacement of beam and column shown in the figure is the average displacement of beams and columns in the compartment. It can be seen in the figure that the displacements of the column, beam, and floor increase sharply at 162 min after the exposure, indicating the collapse of the compartment. The collapse also led to the drop of the floor above the fire compartment.

The structural response of S2 is shown in Fig. 10. It can be seen in Fig. 10(a) that the deformation of the corner column (protected, column 1) is much smaller than the unprotected column (column 2). Therefore, the compartments above the fire location do not drop like S1. The corner compartment subjected to fire still provides enough space for evacuation. Fig. 10(b) exhibits the stress distribution of the building. Due to the load redistribution, the stress of the column near the failed column is higher. Fig. 10(c) shows the displacement evolutions of protected and unprotected column and floor. The maximum displacement of the floor was 5.53 mm and no sharp increase was observed during exposure. It can be concluded that S2 prevented the collapse of the building.

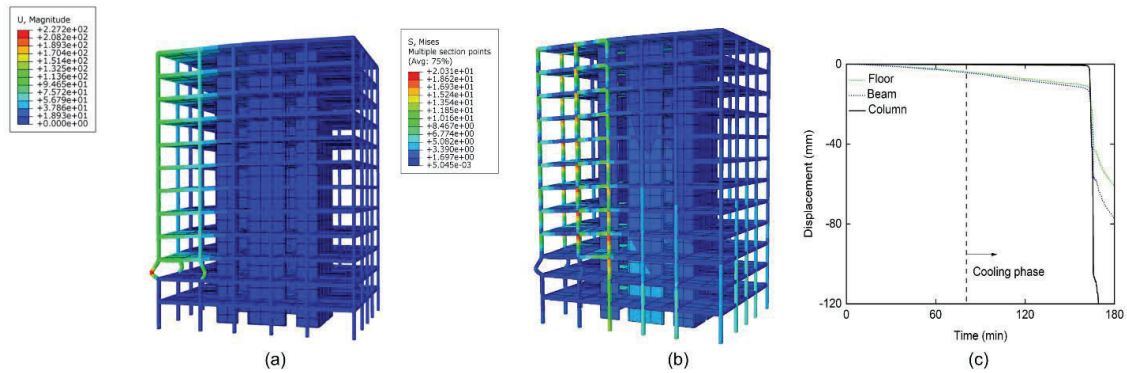


Figure 9. Structural response of S1: (a) deformation mode, (b) stress distribution, and (c) displacement evolutions of components.

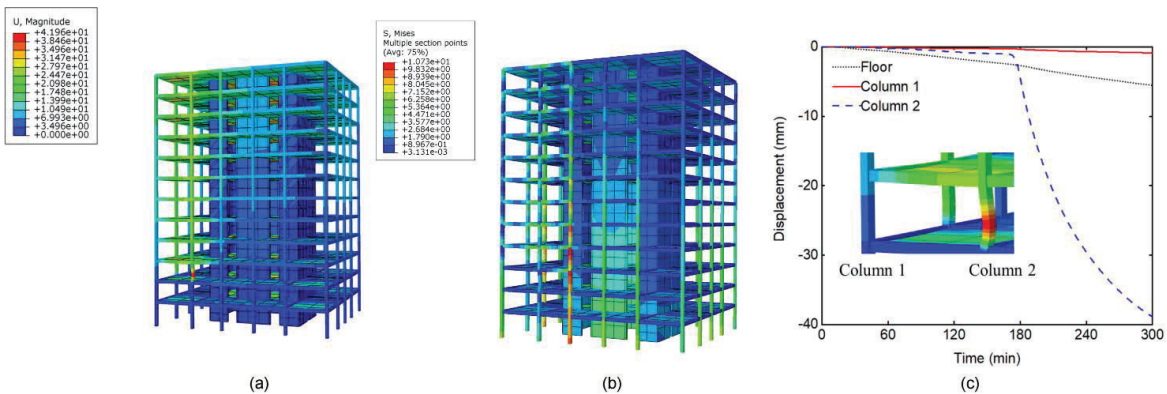


Figure 10. Structural response of S2: (a) deformation mode, (b) stress distribution, and (c) displacement evolutions of components.

4.2 ROBUSTNESS ASSESSMENT

The robustness of S1 and S2 were assessed. The location of fire hazards was assumed to be randomly located on different stories except for story 1 which was assumed to be a public area. Therefore, for each fire hazard scenario i , the possibility of occurrence was the same. And it is reasonable to deduce that once the building survived under fire hazard at i th story, it could survive under fire hazards at $(i + 1)$ th story since the load was smaller for the later case. For S1, the simulations were conducted for the fire scenario located at story 2 to i , and the results are shown in Fig. 11. For the fire scenario located at story 3, the structural response had been analyzed and is not presented in the figure.

It can be seen from Fig. 10 that the building collapses when the fire hazard occurs in story 2 to story 7, and the

building maintains stability when the fire hazard occurs in story 8. For every collapsed scenario, the fire compartment at story i collapses due to the buckling of columns, and compartments from story $i + 1$ to 12 also collapse due to the inclination of the floor. Therefore, the direct failure area equals the floor area of the fire compartment, and the indirect failure area equals the summation of the floor area of story $i + 1$ to the floor area of story 12. Based on Eq. 2, the robustness index I_{rob} for design strategy S1 is 0.52. For design strategy S2, the building did not collapse when the fire scenario occurred in story 2. Therefore, the robustness index I_{rob} for design strategy S2 is 1, indicating its excellent robustness. Compared with S1, the building designed with S2 was more robust under natural fire scenarios, which demonstrated the importance of protecting critical elements during fire exposure.

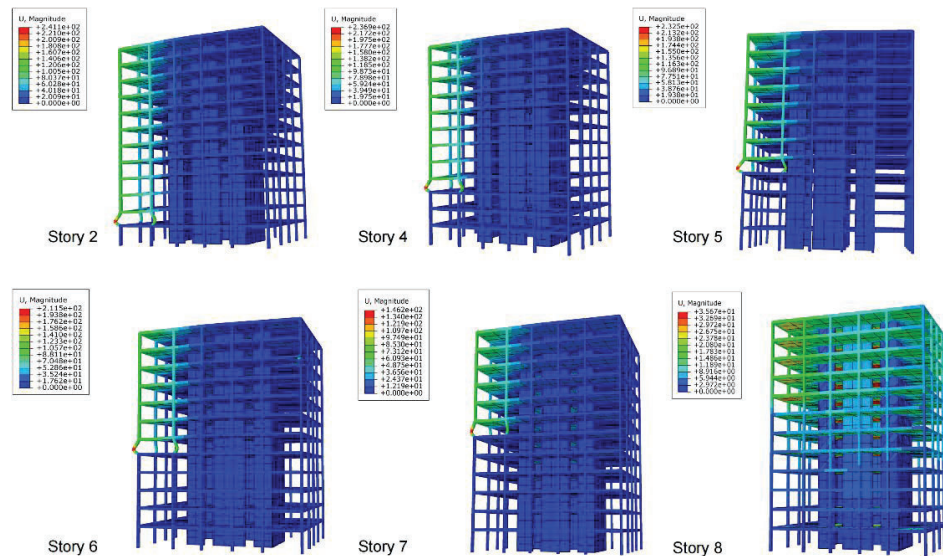


Figure 21. Robustness assessment of S1.

6 – CONCLUSION

This study investigated the structural fire performance and robustness of the high-rise timber building under natural fire scenarios. To simulate the realistic compartment fire evolution, the combustibility of timber was considered through exposed timber surfaces. An iterative calculation procedure was used to determine the contribution of the exposed timber to the total fuel load. The HRR curve was calculated based on the extended fire duration model. The fire curve was obtained based on the calculated HRR curve and Zone model. Sequential thermal-structural analysis was conducted on a numerical building model to evaluate the structural fire performance and assess the robustness of the building based on the collapse scenarios.

Two passive fire protection strategies were considered for the timber building, i.e., no fire protection in S1 and protected diagonal columns in S2. The structural fire performance for S1 indicated that the compartment collapse was due to the buckling failure of columns. The floor dropped, leading to the collapse of compartments above the fire compartment. For S2, however, the protected columns supported the compartment and prevented the collapse. The robustness of the two design strategies were quantified by the direct and indirect collapse area. The fire hazards were assumed to be randomly located at stories 2 to 12. The robustness index of S1 is 0.52 and the robustness index of S2 is 1.0. The structural fire performance and robustness of the timber building indicated that: (1) the timber column was the most vulnerable member under fire exposure; (2) the fire

protection on critical structural elements could significantly improve the robustness of the building.

7 – REFERENCES

- [1] Han, Tongchen, and Solomon Tesfamariam. "Numerical analysis of CLT shear walls using high-fidelity model: Connection to building system." In: *Journal of building engineering* 72 (2023): 106458.
- [2] Han, Tongchen, et al. "Hysteretic behavior of a cross-laminated timber building incorporating different energy dissipators." In: *Soil dynamics and earthquake engineering* 188 (2025): 109038.
- [3] National Research Council Canada. National building code of Canada. Associate Committee on the National Building Code, National Research Council, 2020
- [4] Han, Tongchen, and Solomon Tesfamariam. "Reliability analysis of timber columns under fire load using numerical models with equivalent section temperature." In: *Engineering structures* 324 (2025): 119345.
- [5] Han, Tongchen, and Solomon Tesfamariam. "Component-based modelling of timber beam-column moment connection exposed to fire." In: *Journal of performance of constructed facilities* (2025) (Accepted).
- [6] EN 1991-1-2. "Eurocode 1: Actions on structures - Part 1-2: General actions - Actions on structures exposed to fire." The European Union Per Regulation, 2002.

[7] Brandon. "Fire safety challenges of tall wood buildings—phase 2: Task 4—engineering methods." NFPA, 2018.

[8] Brandon, D. "Practical method to determine the contribution of structural timber to the rate of heat release and fire temperature of post-flashover compartment fires". NFPA, 2016.

[9] McGregor, C. "Contribution of cross laminated timber panels to room fires." Ph.D. thesis. Carleton University- Department of Civil Engineering, 2013.

[10] Ni, S. and Gernay, T. "On the effect of exposed timber on the severity of structural fires in a compartment and required firefighting resources." In: Fire technology, 58(5), 2691–2725.452, 2022.

[11] Voulpiotis, Konstantinos, et al. "A holistic framework for designing for structural robustness in tall timber buildings." In: Engineering structures 227: 111432, 2021.

[12] Voulpiotis, Konstantinos, Styfen Schär, and Andrea Frangi. "Quantifying robustness in tall timber buildings: A case study." In: Engineering structures 265: 114427, 2022.

[13] Starossek, Uwe, and Marco Haberland. "Approaches to measures of structural robustness." In: Structure and infrastructure engineering 7.7-8: 625-631, 2011.

[14] Baker, Jack W., Matthias Schubert, and Michael H. Faber. "On the assessment of robustness." In: Structural safety 30.3: 253-267, 2008.

[15] Cadorin, J., Pintea, D., and Franssen, J. "The design fire tool ozone v2. 0-theoretical description and validation on experimental fire tests." Rapport interne SPEC/2001_01 University of Liege, 2001.

[16] EN 1994-1-2. "Eurocode 5: Design of Timber Structures—Part 1–2: General—Structural Fire Design." The European Union Per Regulation, 2004.

[17] Gagnon, S. and Pirvu, C. "CLT handbook: cross-laminated timber." FPInnovations, 2019.